UMYU Scientifica, Vol. 5 NO. 1, March 2026, Pp 423 – 432
https://doi.org/10.56919/usci.2651.036
ISSN: 2955 – 1145 (print); 2955 – 1153 (online)
A periodical of the Faculty of Natural and Applied Sciences, UMYU, Katsina

ORIGINAL RESEARCH ARTICLE

Adsorption Performance of Raw Water Lily (*Nymphaea lotus*) Leaves for Methyl Violet Removal: Kinetics, Isotherms and Thermodynamic Studies

Hamisu Abdulmumini*[1], Abdullahi Muhammad Ayuba[2], Ahmad Hashim Umar[4], Buhari Labaran[4], Aishat Ahmad Tijjani[3], Sulaiman Umar Abubakar[4]

[1]Department of Chemistry, Abubakar Tafawa Balewa University, PMB 0248, Ningi/Kano Road, Bauchi-Nigeria
[2]Department of Pure and Industrial Chemistry, Bayero University, PMB 3011, Kano-Nigeria
[3]Department of Medical Biochemistry, Abubakar Tafawa Balewa University, PMB 0248, Ningi/Kano Road, Bauchi-Nigeria
[4]Department of Science of Science Laboratory Technology, Abubabar Tatari Ali Polytechnic, PMB 0094 Bauchi-Nigeria

ABSTRACT

The Discharge of methyl violet effluents from textile and other related industries poses serious environmental and health problems due to its toxicity, non-biodegradable and it persistent in water bodies. Adsorption is considered as an effective and economical method for dye removal. However, the development of efficient, low cost and sustainable adsorbents is still a challenge. In this study, raw water lily (*Nymphaea lotus*) leaves powder was prepared and used as adsorbent for the adsorption of methyl violet (MV) dye from aqueous solution. A Batch adsorption experiment was conducted to investigate the effect of contact time (15-150min), dosage (20-200mg), initial concentration (30-180mg/L) and pH (3-13) respectively. The adsorbent was characterised using scanning electron microscope (SEM) and Fourier transform infrared (FT-IR) spectroscopic methods. Langmuir, Fruendlich, Temkin and DRK isotherm models, as well as pseudo-first order, pseudo-second order, elovich and intraparticles diffusion models were studied and applied. And finally thermodynamic parameters were also evaluated. The results showed that the best adsorption of MV onto RWL was at 90min contact time, 100mg adsorbent dosage, concentration of 90.00mg/L and the pH of 13 were taken as the optimised conditions. The equilibrium data generated shows that Temkin model best fitted/described the adsorption process with regression value (R2 =0.9586) close to unity. The heat of adsorption was estimated from Temkin isotherm model to be 0.240kJ/mol and mean free energy was estimated from Dubinin-Rudushkevich (DRK) model to be 0.121kJ/mol indicating the adsorption process to obey chemisorption mechanism. The kinetic data generated revealed that the adsorption process of MV onto the RWL adsorbent followed pseudo-second-order kinetics, with R^2 values of 0.9978. The experimental qe (241.80mg/g) and calculated adsorption capacity qcal (232.56mg/g) were in agreement. The thermodynamics studies conducted revealed that the adsorption was spontaneous and feasible with Gibbs' free energy change (ΔG) values ranging from -10.37 to -11.30kJ/mol, exothermic in nature with enthalpy change (ΔH) value of -1.03kJ/mol and entropy change (ΔS) during transfer of molecules between the solid and liquid phase with entropy to be 30.8J/mol. This study reveals the potentials of RWL as a promising adsorbent for the removal of MV dye from aqueous solutions.

ARTICLE HISTORY

Received December 03, 2025
Accepted March 15, 2026
Published March 28, 2026

KEYWORDS

Methyl Violet, Thermodynamics, Adsorption, Kinetics, Isotherms

INTRODUCTION

Dyes are organic compounds with both hydrophilic and hydrophobic linkages; these chemical dyes pollute natural water bodies and have been used for both domestic and industrial purposes (Abrishamkar *et al.,* 2020). It's estimated that about 5-10 percent of chromogenic materials discharged into streams and water bodies are disposed of by the textile industries. Color is the first contaminant to be recognized in wastewater, even at minute concentrations (1.0 mg/L), and is highly visible, affecting the aesthetic merit, transparency, and gas solubility of water bodies (Bonetto *et al.,* 2015). They are non-biodegradable, generally immutable, and persistent in the environment (Abisola *et al.,* 2020).

Methyl violet (MV), a basic dye with a brilliant hue and intensity, has found usage in the textile, paint, and printing ink manufacturing industries (Mittal *et al.,* 2007; Dahri *et al.,* 2013), in biomedical fields, it's an active ingredient in Gram's staining for bacteriological applications and a moderately effective disinfectant (Ali *et al.,* 2022; Muhd

Correspondence: Hamisu Abdulmumini. Department of Chemistry, Abubakar Tafawa Balewa University, PMB 0248, Ningi/Kano Road, Bauchi-Nigeria. ✉ ahamisu@atbu.edu.ng.

How to cite: Abdulmumini, H., Ayuba, A. M., Ahmad, H. U., Labaran, B., Ahmad, A. T., & Umar, S. A. (2026). Adsorption Performance of Raw Water Lily (*Nymphaea lotus*) Leaves for Methyl Violet Removal: Kinetics, Isotherms and Thermodynamic Studiea. *UMYU Scientifica*, 5(1), 423 – 432. https://doi.org/10.56919/usci.2651.036

Din *et al.,* 2009). Toxicological information indicates that the dye may cause skin and eye irritation, redness, and pain; inhalation and ingestion may also cause irritation of the respiratory and gastrointestinal tracts, respectively, and therefore warrant its eradication from the ecosystem (Muh'd Din *et al.,* 2010).

A wide range of studies has been conducted on chemical, biological, and biochemical processes to treat dye-contaminated wastewater. These include membrane processes, coalescence-based methods, ion exchange, oxidation processes, ozonation techniques, photocatalysis, chemical deposition, and adsorption (Sharafzad *et al.,* 2021). Among others, adsorption is an effective method of dye removal due to its low cost, low energy usage, and high efficiency (Duan *et al.,* 2012), while materials that can be recycled and reused are considered an added advantage. In the adsorption process, a dye molecule is adsorbed onto the biomass via physical or chemical adsorption, thereby avoiding the formation of degraded dye products that may be more harmful than the original dye itself (Dahri *et al.,* 2013). Therefore, adsorption using renewable biomass has a key advantage over non-renewable adsorbents, such as clay, peat, zeolite, and lignite.

Literature has reported the use of agricultural biomass as an effective adsorbent for the removal of methyl violet dyes from aqueous solutions. Some of which include the use of *Sapindus mukorossi* (Samal *et al.,* 2019), pecan pericarp (*Carya illinoensis*) (Yamil *et al.,* 2020), date palm fronds waste (Zubair *et al.,* 2020), palm kernel activated carbon (Mehr *et al.,* 2020), *ipomoea aquatica* roots (Lu *et al.,* 2021), calcined lotus leaf (Sharafzad *et al.,* 2021), date seeds (Ali *et al.,* 2022), rice husk powder (You *et al.,* 2022), activated carbon Oak wood (Foroutan *et al.,* 2022), *hagenia abyssinica* leaf powder (Geremew *et al.,* 2022), *parkia speciosa hassk* peel (Syakina & Rahmayanti, 2023). Our literature search did not find the use of raw water lily leaves as an adsorbent for the removal of methyl violet from aqueous solutions.

Accordingly, this study aims to explore the potential of raw water lily (RWL) leaves as low-cost adsorbents for the removal of methyl violet from aqueous solutions under optimized conditions, including contact time, dosage, initial concentration, pH, and temperature. Parameters describing the adsorption process, including isotherms, kinetic models, thermodynamic parameters, and surface characterization, were also investigated and reported.

MATERIALS AND METHODS

2.1 Chemicals, Reagents, and Apparatus

All the chemical reagents and materials used in this research were of analytical grade and were collected and used without any further purification: sodium hydroxide (NaOH), hydrochloric acid (HCl), pestle and mortar, beakers, conical flask, volumetric flask, sieve, distilled water, filter paper (Whatmann No. 1), funnels, glass rod, and methyl violet (MV) dye, UV-visible spectrophotometer.

2.2 Sample Collections and Adsorbent Preparation

The adsorbent was prepared according to the method described by Oznur *et al.* (2013). The water lily leaves (WLL) were obtained from Gubi Dam, Bauchi State, Nigeria. The leaves were washed thoroughly with distilled water to remove dust impurities and shade-dried for 72 hours. The dried leaves were ground and sieved to a working size of 300 µM, and the resulting raw leaf sample (RWL) was stored in an airtight container.

2.3 Preparation of Stock Solution

A stock solution of methyl violet dye (Fig 1) was prepared by dissolving 1 g of the dye in a 1000 mL volumetric flask at room temperature, shaking until a homogeneous solution was obtained, to obtain a concentration of 1000 mg/L (Ibrahim & Sani, 2015). The sample of required concentration was prepared by diluting the stock solution with distil water to the required concentration using the dilution formula in equation (1):

$$C_1V_1 = C_2V_2 \quad \text{.....} \quad (1)$$

Where C_1 and C_2 are the initial and final concentrations, V_1 and V_2 are the initial and final volumes.

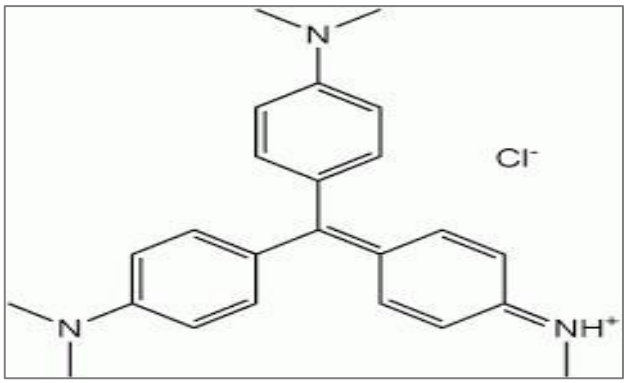

Fig 1: Structure of methyl violet dye

2.4 Optimization of Experimental Parameters

2.4.1 Effect of Contact Time

The effect of contact time on the adsorption of the MV dye used in this experiment was studied at room temperature, with an initial concentration of 100 mg/L. An adsorbent dose of 100mg of raw adsorbent was introduced and shaken for the following time intervals: 15, 30, 60, 90, 120, and 150 minutes at 150 rpm (Malik *et al.,* 2007).

2.4.2 Effect of Dosage

The effect of dosage was assessed according to the method described by Manjunatha & Vagish (2016). The effect of adsorbent dosage was studied at an initial concentration of 100 mg/L with adsorbent dosages of 0.02 g, 0.05 g, 0.08 g, 0.1 g, and 0.2 g, respectively. The weighed samples were taken in polythene bottles with 50 mL of the stock solution. The samples were kept in an orbital shaker at room temperature at a constant speed of 150 rpm for the determined optimum time.

2.4.3 Effect of Initial Concentration

Concentration is among the important factors influencing the rate of chemical reactions. The effect of varying the initial concentration of the MV dye solution at room temperature, using a fixed amount of adsorbent, was determined at 30, 60, 90, 120, 150, and 180 mg/L. The mixture was then shaken for the optimal time at room temperature with an adsorbent dosage of 0.02 g at 150 rpm. The solution was filtered using Whatman filter paper, and the filtrate was then analyzed by UV-spectrophotometry (Zhai *et al.,* 2020).

2.4.4 Effect of pH

The adsorption experiment was carried out at different pH values to determine the optimal pH for adsorption. The optimum initial concentration and adsorbent dosage were added to five different polythene bottles (50 mL), each conditioned at a different pH (3, 5, 7, 9, 11, and 13) at room temperature. The pH was adjusted to the desired value with 0.1 M HCl or 0.1 M NaOH, respectively. The bottles were shaken at 150 rpm and then filtered. The filtrate was analyzed using a UV-spectrophotometer to determine the residual (unadsorbed) concentration of the dye (Majithiya *et al.,* 2013; Oznur *et al.,* 2013).

2.5 Adsorption Equilibrium Experiments

For this experiment, batch adsorption was adopted due to its simplicity, as reported by Shahryari *et al.* (2010). Batch experiments were conducted to determine the optimal conditions for the equilibrium adsorption of MV dyes onto RWL. The results from the optimization experiments were used to conduct batch adsorption under ideal conditions. These systems were run separately in 60 cm3 polythene sample bottles at 30, 40, 50, and 60 °C, respectively. The samples were placed in temperature-controlled shakers for the period reported for each system. After reaching equilibrium, the filtrate was analyzed using a Perkin-Elmer UV-visible Spectrophotometer at a maximum absorbance wavelength of 582.37 nm. The amount of the adsorbed dye was obtained using equation (2).

$$q_e = \frac{(C_o - C_e)}{m} x\, V \quad \text{...(2)}$$

While the color removal rate (% Removal) was calculated using equation (3):

$$\%R = \frac{(C_o - C_e)}{C_o}\, x\, 100 \quad \text{.....................................(3)}$$

Where: q_e is the adsorption capacity (mg/g), C_o and C_e are the initial and final concentrations in mg/l) respectively for the dye in the solution, V is the volume of the dye in the solution (L), and m (g) is the mass of the adsorbent (Ibrahim & Sani, 2015; Shahryari *et al.,* 2010).

2.6 FT-IR Analysis

Fourier transform infrared spectroscopy was used to study the surface functional groups present in the adsorbent before and after adsorption of MV, so that an idea of the functional groups present in the adsorbent could be inferred. IR spectra were obtained with a PerkinElmer Spectrum 100 FTIR spectrometer (Agilent Technologies, USA) using 20 scans at a spectral resolution of 4 cm-1 by the attenuated total reflectance method. FTIR spectra were collected in the mid-infrared region between 4,000 and 650 cm^{-1}. All spectra were acquired using air background correction (Anisuzzaman *et al.,* 2015).

2.7 Scanning Electron Microscope (SEM) Analysis

Scanning electron microscopy (SEM) is used to analyze the surface morphology of the adsorbent and was performed by viewing electron micrographs of the studied adsorbent (Sartape *et al.,* 2017). The analysis was performed using a proxy scanning electron microscope (Phenom World, Eindhoven). For SEM analysis, a thin layer of adhesive, serving as carbon glue, was attached to a stub, and a very small amount of the material to be viewed was spread on the stub and subsequently viewed in the instrument to obtain micrographs. Scanned micrographs of RWL before and after adsorption were taken at an accelerating voltage of 15 kV and 1500X magnification.

RESULTS AND DISCUSSION

3.1 Surface Characterization of Bio-sorbents

To investigate the surface morphology of RWL, SEM analysis was performed. Figs. 2 (a and b) show the surface of the biosorbent both before and after adsorption of MV dye. The SEM micrograph in Fig. 2a shows cavities with wide cracks and some spongy-like portions that may aid adsorption. After adsorption of MV onto RWL, as presented in Fig. 2b, the figure shows the deposition of MV dye molecules onto the surface of the RWL, which results in the formation of a relatively more homogeneous surface with filled cracks, pores, and rough surfaces. This shows that an interaction between the MV dye molecules and the adsorbent surface apparently occurs through adsorption.

However, the FT-IR spectroscopic analysis was used to determine the presence of functional groups in RWL before and after adsorption of MV dye molecules, as shown in Fig 3. The presence of hydroxyl groups on the biomass surface was inferred from the strong, broad peaks observed at 3444 and 3286 cm^{-1}. The peaks at 2950 and 2921cm^{-1} refer to C-H functional groups, while the peaks observed after adsorption at 2102 and 1369cm^{-1} were attributed to alkynes and C-O functional groups, which were all absent before adsorption of the dye. This could be attributed to the presence of a new functional group, formed by the formation of new bonds. However, peaks at 1632 and 1637 cm^{-1} and at 1405 and 1588 cm^{-1} were attributed to the carboxylic group and the aromatic functional group, respectively, both before and after adsorption of the dye. Additionally, peaks at 1080 and 1022 cm^{-1} are associated with the C-H aromatic functional group. Many researchers have established that functional groups from both dyes and adsorbents participate in the adsorption process (Oyeyode & Ayuba, 2022; Karim *et al.,* 2017).

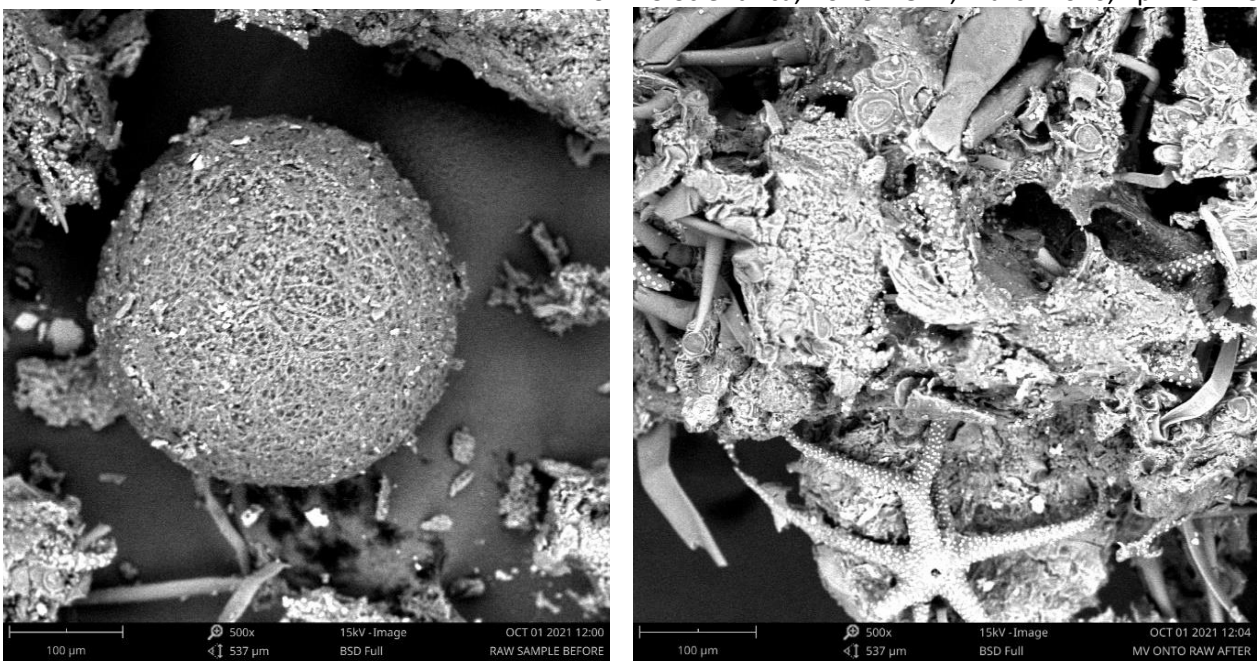

(a) **(b)**

Fig 2: SEM micrograph (b) before adsorption of MG (b) after Adsorption of MG

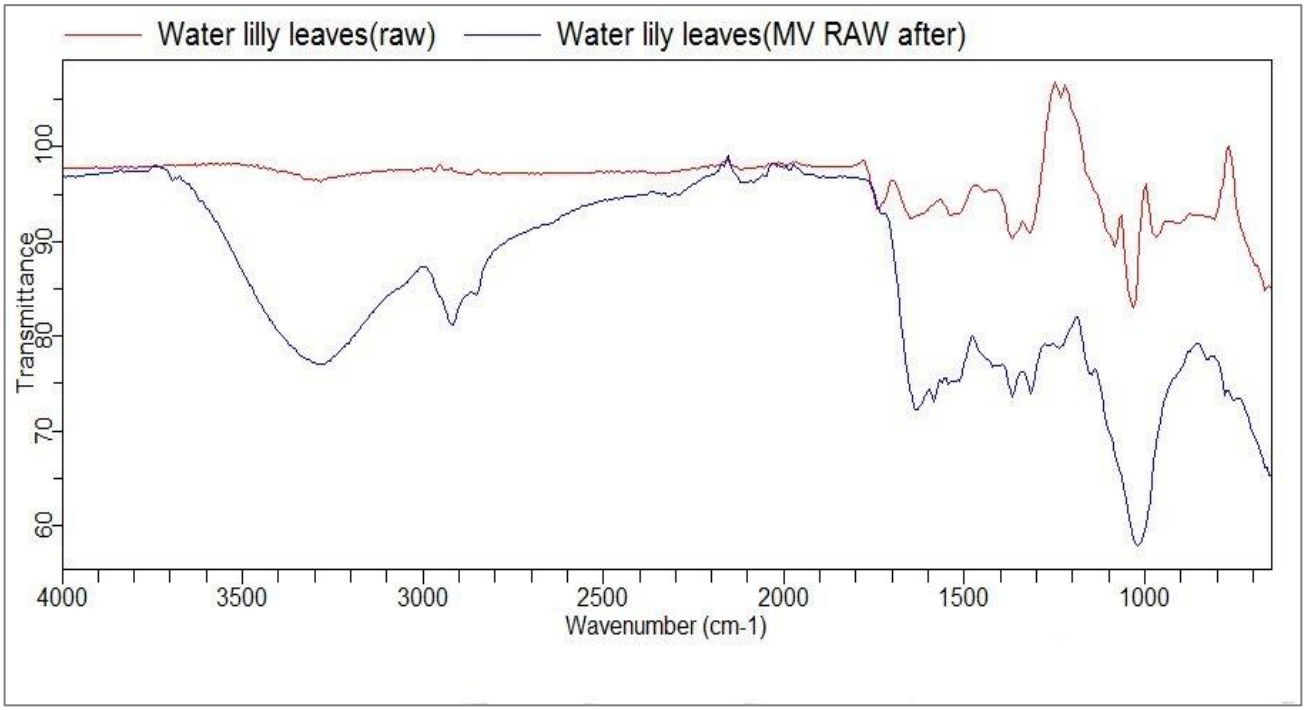

Fig 3: FT-IR Spectra before and after adsorption of MV

3.2 Optimization Studies

Fig. 4(a) demonstrates the effects of contact time on the adsorption of MV onto the RWL adsorbent by varying the contact time from 15 to 150 minutes at room temperature with an initial concentration of 100 mg/L. The initial MV uptake was rapid during the first 15–90 minutes and subsequently declined thereafter. The higher sorption rate observed during the initial period of the process could be partly attributed to the presence of a large number of vacant sites on the adsorbent surface, which facilitates rapid adsorption and the accommodation of MV molecules. After a time lapse (90 min), the large vacant sites of RWL that were available at the beginning of the adsorption of MV from the solution had become rarely accessible or exhausted after establishing equilibrium (Naghizadeh *et al.,* 2011; Giwa *et al.,* 2018). Later on, the process becomes relatively slower, as the equilibrium conditions are reached, whereas the amount of MV desorbing from the adsorbent is in a state of dynamic equilibrium with the amount of MV being adsorbed onto the adsorbent surface. Similar trends were reported by Hameed and El-Khaiary (2008).

Fig 4b shows a plot for the variation of the adsorbed amount of MV with the adsorbent dosage of RWL. It was studied by varying the amount of adsorbent from 20 to 200mg, while other parameters were kept constant. It was

revealed that the amount of MV adsorbed decreased per unit mass with increasing dosage, partly due to limited accessibility, saturation, or even possible overlapping of the adsorbent's active binding sites for MV binding as the adsorbent dosage increased. This will equally reduce the effective adsorption process (Ayuba & Thomas, 2019). Similar trends were reported by some researchers (Bedmohat *et al.,* 2015; Yusuff, 2019).

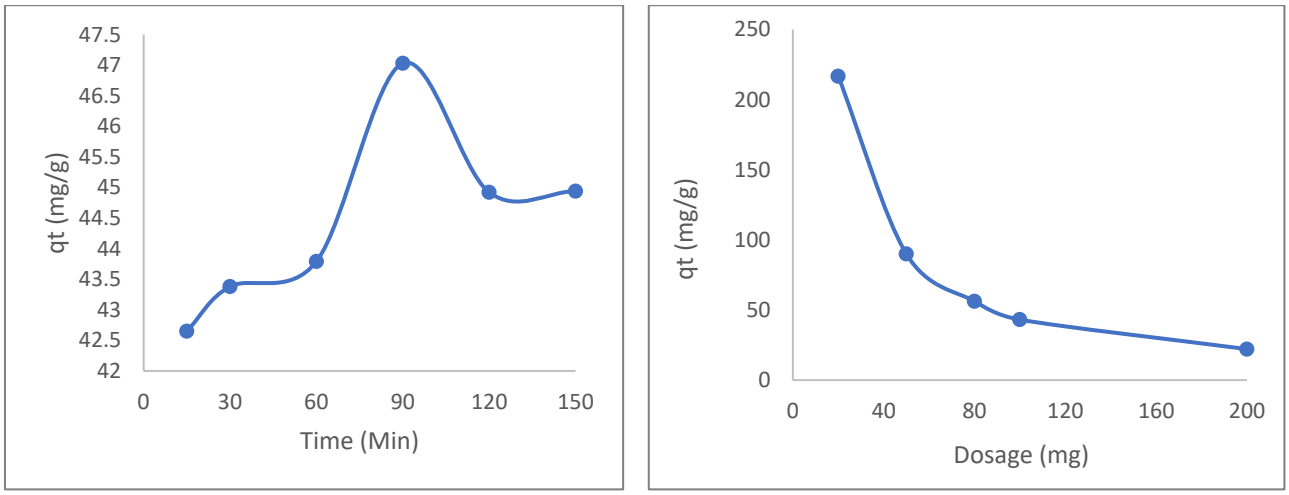

(a) **(b)**

Fig 4: Effect of (a) Contact Time, (b) Dosage on adsorption of MV onto RWL adsorbent

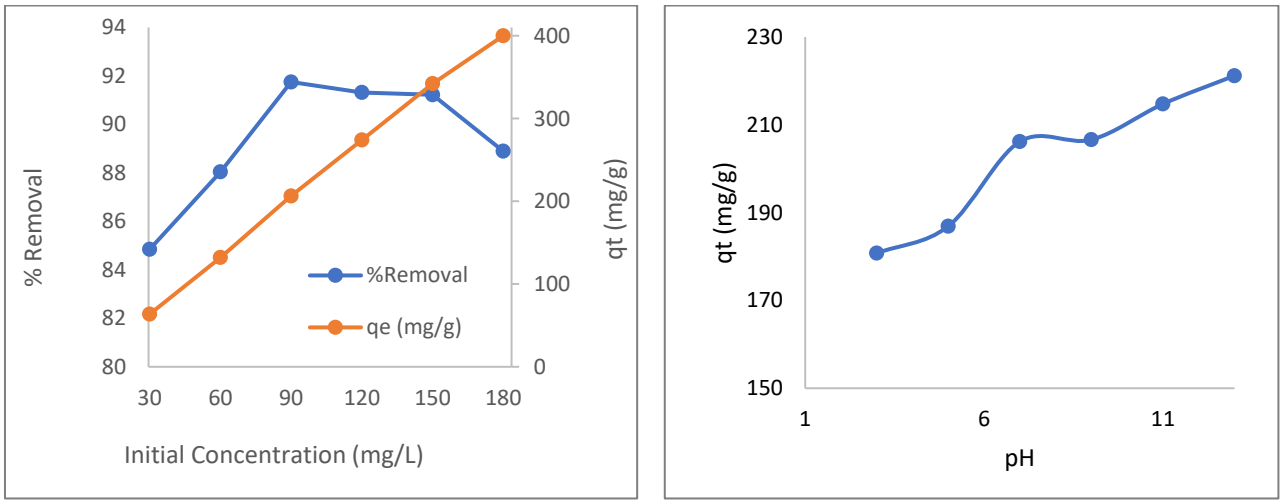

(a) **(b)**

Fig 5: Effect of (a) Initial Concentration (b) pH on adsorption of MV onto RWL adsorbents

Table 1: Calculated isotherm parameters for the adsorption of Methyl violet onto RWL adsorbent

Isotherms	Parameters	Values
Langmuir	q_0 (mg/g)	321.50
	K_L(L/mg)	24.69
	R_L	0.121
	R^2	0.8982
Freundlich	1/n	1.2394
	N	0.8068
	K_F	12.572
	R^2	0.8817
Temkin	A_T	0.2868
	b_T	10.33
	B	239.81
	R^2	0.9586
D-R	qs(mg/g)	418.217
	β(mol^2/kj^2)	8.0×10^{-8}
	c (kJ/mol)	0.121
	R^2	0.9497

Table 2: Kinetic models parameters for the adsorption of MV onto RWL

Kinetic Model		Parameters			
Pseudo-first order		Q_{exp}(mg/g)	Q_{cal}(mg/g)	k_1(min^{-1})	R^2
	30^{0}C	241.80	3.97	-1.61x10^{-2}	0.4573
	40^{0}C	221.42	6.26	-1.98x10^{-2}	0.0879
	50^{0}C	190.26	5.76	8.71x10^{-2}	0.3651
Pseudo-first order		Q_{exp}(mg/g)	Q_{cal}(mg/g)	k_2(mg/gmin)	R^2
	30^{0}C	241.80	232.56	2.64x10^{-2}	0.9960
	40^{0}C	221.42	196.08	2.99x10^{-3}	0.9934
	50^{0}C	190.26	188.68	5.40x10^{-3}	0.9978
Elovich model			B	A	R^2
	30^{0}C		-0.268	-3.68	0.1542
	40^{0}C		-0.183	-5.33	0.2400
	50^{0}C		0.222	-4.63	0.4654
Intraparticle diffusion			C	K_{int}	R^2
	30^{0}C		241.92	-1.43	0.1209
	40^{0}C		224.19	-2.82	0.3414
	50^{0}C		170.96	2.08	0.5331

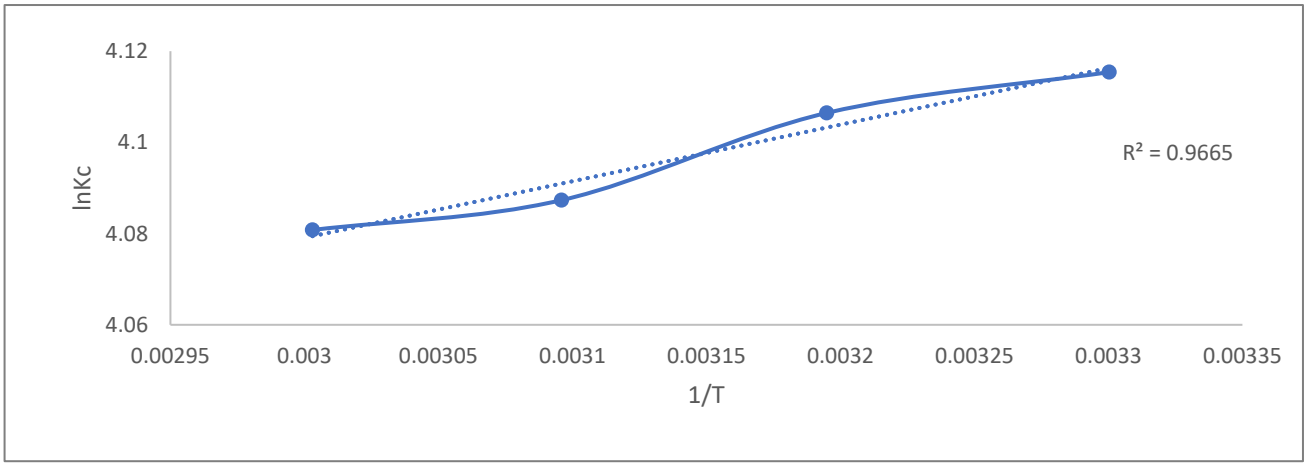

Fig 6: The Van't Hoff Plot for adsorption of MV-RWL

Table 3: Thermodynamics parameters

T(K)	ln K_c	ΔG (kJ/mol)	ΔH (J/mol)	ΔS (J/mol.K)
303	4.115	-10.367	-1.032	30.817
313	4.087	-10.686		
323	4.081	-10.976		
333	3.361	-11.298		

Fig 5a shows a plot of the variation of the amount of MV adsorbed with respect to the initial concentration. From the plot, the amount of MV adsorbed by RWL increases with increasing concentration. At lower concentrations, the available driving force for the transfer of MV molecules onto RWL is low, while at higher concentrations, there is an increase in driving force, which in turn enhances the interaction between the MV molecules in the aqueous phase and the vacant active sites of the RWL, hence the increase in the MV uptake (Abdul-Salam & Adekola, 2018). The percent removal increases gradually at lower concentrations, reaches a maximum, and then rapidly decreases. This is because vacant or active sites on the RWL surface become saturated or become inaccessible to MV molecules (Ullah *et al.,* 2021).

The effect of pH was studied by varying the pH from 3 to 13 while keeping other operating parameters constant. A plot of the variation in the amount of MV adsorbed is shown in Fig. 5b. The amount of MV adsorbed by RWL increases significantly as the pH of the solution is adjusted from acidic to basic. This case is typical, as most studies show that adsorbate removal increases with increasing pH (Dahri *et al.,* 2013; Li *et al.,* 2010; Chakraborty *et al.,* 2011).

3.3 Isotherms Studies

In this study, equilibrium data were generated and analyzed using four fundamental isotherms, viz., the Langmuir, Freundlich, Temkin, and D-R models. These models are used to describe the adsorbent-adsorbate behavioral interaction and to understand the mechanism of the adsorption pathways.

(a) Langmuir Isotherm

According to this model, the adsorption of analytes assumes or takes place on homogenous sites of the adsorbent's surface with monolayer formation (Ullah *et al.,* 2021) and can be expressed as:

$$\frac{1}{q_e} = \frac{1}{q_0} + \frac{1}{q_0 K_L C_e} \quad \text{.....(4)}$$

Where q_e is the amount of MV retained at equilibrium by the adsorbent in mg/g, q_0 is the monolayer adsorption capacity (mg/g), K_L is the Langmuir constant (L/mg), and C_e is an equilibrium concentration (mg/L), respectively. The K_L and q_0 were determined using the slope and intercept of a graph of $1/q_e$ vs $1/C_e$, and the parameters were computed as shown in Table 2.

The dimensionless separation factor R_L is defined by the relation in equation (5)

$$R_L = \frac{1}{1+K_L C_o} \quad \text{..... (5)}$$

Where C_o is the maximum initial concentration (mg/g).

The R_L indicates whether the adsorption process is unfavorable ($R_L > 1$), linear ($R_L = 1$), favorable ($0 < R_L < 1$), or irreversible ($R_L = 0$).

(b) Freundlich Isotherm

This model described the adsorption process as being irreversible, non-ideal, and resulting in multi-layer coverage on the heterogeneous surface of the adsorbents (Dehgari *et al.,* 2018). This model can be expressed using equation (6)

$$log q_e = log K_f + \frac{1}{n} log C_e \quad \text{..... (6)}$$

Where q_e *is* the quantity of MV adsorbed in mg/g, C_e is the equilibrium concentration of the adsorbates in mg/L, K_f is the Freundlich constant related to maximum adsorption capacity, and n is the Freundlich constant related to maximum adsorption capacity (dimensionless).

(c) Temkin Model

This model considers the interaction between adsorbent materials and adsorbed adsorbate molecules, assuming that the adsorption free energy is a function of surface coverage (Nyijime & Ayuba, 2020). This isotherm is expressed in equation 7.

$$qe = \frac{RT}{bT} \ln At + \frac{RT}{b} \ln Ce \quad \text{..... (7)}$$

where R is the molar gas constant ($Jmol^{-1}K^{-1}$), T is the temperature in Kelvin, b is the variation of adsorption energy (J/Mol), and b_T is the equilibrium binding constant (L/mg) corresponding to the maximum binding energy. The values of and A_T were obtained and tabulated in Table 2 from the slope and intercept of qe against the ln Ce plot, respectively.

(d) Dubinin-Rudushkevich (D-R) isotherm

This model is used to determine the adsorption behavior of MG towards the adsorbate using equation (8) (Nica *et al.,* 2020).

$$\ln q_e = \log q_0 - K \epsilon^2 \quad \text{..... (8)}$$

where q_o is the constant of D-R (mol/g), and K is the mean free energy of adsorption (kJ/mol). However, ϵ can be calculated using equation (9)

$$\epsilon = RTln(1 + \frac{1}{C_e}) \quad \text{..... (9)}$$

where Ce is the adsorbate equilibrium concentration, R is the ideal gas constant (8.314 J/mol.K), and T is the temperature in Kelvin. The values of q_o and K were obtained using the slope and intercept from the plot of $\ln C_e$ against ϵ^2, respectively.

Table 1 shows the Langmuir, Freundlich, Temkin, and D-R isotherm constants for the adsorption of MV onto RWL. The computed R^2 values indicated that the Temkin isotherm model best fit the experimental data for the MV-RWL adsorption process. Both the equilibrium binding constant b_T and the heat of adsorption (β) values were found to be 10.33 L/mg and 239.81 J/mol respectively. As a result, physical adsorption is assumed.

3.4 The Kinetics Studies

A study of adsorption kinetics is desirable, as it provides information on the adsorption mechanism, which is important for the process's efficiency (Lafrano *et al.,* 2016). To understand the process, two kinetic models (i) pseudo-first order model, (ii) pseudo-second order model equations were applied to analyze the experimental data:

(a) Pseudo-first order model

The linearized form of pseudo –first order kinetic model can be written as:

$$\log(q_e - q_t) = \log q_e - \frac{k_1}{2.303} \quad \text{..... (10)}$$

where qe and qt (mg/g) are the amounts of dyes adsorbed at equilibrium and at time t, respectively, and k_1 (min^{-1}) is the rate constant of adsorption. The plot of log (qe-qt) vs. t should yield a linear relationship, from which k1 and qe were determined from the slope and intercept, respectively, as shown in Table 2. The R^2 values were not close to unity, and Q_{cal} was lower than the experimental (Q_{exp}) value at all temperatures, indicating that the pseudo-first-order model did not fit the kinetic data.

(b) Pseudo-second order model

This adsorption kinetics model can be written as;

$$\frac{t}{q_t} = \frac{1}{k_2 q_e^2} + t/q_e \quad \text{..... (11)}$$

Where k_2 is the rate constant of adsorption (g/mg.min), qe and qt are the amounts of dye adsorbed at equilibrium and at time t (mg/g), respectively. The values of k_2 and Q_{cal} were obtained from the intercepts ($1/k_2 q_e^2$) and the slope (1/qe) of the plots t/q_e vs. t, respectively, and presented in Table 3. The correlation coefficient for the pseudo-second-order model was close to unity, and Qcal values computed from the pseudo-second-order equations showed good agreement with the experimental data, indicating the applicability of the pseudo-second-order kinetic model for the RWL-MV system at all experimental temperatures. Therefore, this model fits the kinetic data of the systems.

(c) Elovich Model Equation

This model is described by the following relation in equation (12) (Kayode *et al.,* 2020).

$$q_t = \frac{1}{\beta}\ln(\alpha\beta) + \frac{1}{\beta}\ln t \quad \text{.......... (12)}$$

The parameters α and β are the initial rate constant (mg/g.min) and desorption constant, respectively, which can be calculated from the slope and intercept of the linear plot of q_t vs ln t. This model provides useful information on the extent of both surface activity and the adsorption activation energy (Ayuba & Hamisu, 2022). The R^2 values obtained for this model were all ≤ 0.4654 at all experimental temperatures. These deviations from linearity (R^2 not close to unity) suggest that this model does not fit the kinetic data.

(d) Intraparticle Diffusion Equation

The possibility of using the intraparticle diffusion model as the sole mechanism was investigated using the Weber-Morris equation (13) (Ayuba & Thomas, 2019).

$$q_e = C + kln\, t^{1/2} \quad \text{..........(13)}$$

where the constant k_{int} (mg/g.min.) is the intra-particle diffusion constant ratio, and C is the boundary layer thickness. If the rate-limiting is only due to intraparticle diffusion, then q_t vs $t^{1/2}$ gives a linear plot that passes through the origin. Otherwise, other mechanisms or factors, in addition to the intraparticle diffusion mechanism, may be responsible. From Table 3, it is evident that the intra-particle diffusion model is not applicable for the adsorption of MV onto RWL adsorbents, since q_t vs $t^{1/2}$ does not pass through the origin. It can be concluded that intraparticle diffusion may not be the sole rate-determining step of the adsorption mechanism.

3.5 Thermodynamic Studies

To estimate the effect of temperature on the adsorption of methyl violet dye onto the RWL adsorbent, thermodynamic parameters such as changes in Gibbs' free energy (ΔG), enthalpy (ΔH), and entropy (ΔS) were evaluated using equations (14, 15, and 16)

$$K_c = \frac{C_s}{C_e} \quad \text{..........(14)}$$

$$\Delta G = -RTlnK_c \quad \text{..........(15)}$$

$$lnK_c = -\frac{\Delta H}{RT} + \frac{\Delta S}{R} \quad \text{..........(16)}$$

The ΔH and ΔS functions were determined from the slope and the intersection point of ln K_c versus the 1/T plot (Figure 6). Whereas C_s is the amount of adsorbate in the adsorbed phase and C_e signifies the remaining un-adsorbed MV concentration (mg/L) in the liquid phase at equilibrium time, T and R are temperature (K) and molar gas constant (8.314Jmol^{-1}k^{-1}).

The values of the thermodynamic parameters obtained were reported in Table 3. Generally, a negative ΔG value indicates the spontaneity and feasibility of MV adsorption onto the RWL adsorbent. However, the negative values of ΔG increase with increasing temperature, indicating the adsorption of MV-RWL to be conducive at higher temperatures [46]; The negative values of ΔH (-1.021J/mol) manifest that the adsorption of MV onto RWL is an exothermic process and corresponds to physio-sorption (ΔH<10kJ/mole), while the positive value of ΔS implies the randomness at the solid/liquid interface during the adsorption of MV-RWL which results in increasing MV concentration at the solid/liquid interface (Belala *et al.,* 2011; Zai *et al.,* 2020).

CONCLUSION

This work shows that the raw water lily leaf-derived adsorbent was an effective adsorbent for the adsorption of methyl violet from aqueous solution. The characterization of the adsorbent surface using FTIR and SEM before and after adsorption confirmed the functional groups on the adsorbent's surface responsible for the adsorption process. The adsorption of the methyl violet dye was found to be affected by changes in contact time, adsorbent dosage, initial MV concentration, and pH. Kinetically, the MV adsorption onto CWL was found to follow the pseudo-second-order kinetic model, while the Temkin adsorption isotherm best describes the mechanism. Thermodynamic studies confirmed that the process was spontaneous, exothermic, and increased the system's randomness at the adsorbent-liquid interface.

FUNDING

This Research received no funding.

ACKNOWLEDGEMENTS

The authors are grateful to Bayero University Central Laboratory and Abubakar Tatari Ali Polytechnic, Bauchi, both in Nigeria, for providing facilities for this study.

CONFLICT OF INTEREST

The authors declare no conflict of interest

REFERENCES

Abdul-salam N., Adekola S.K., (2018). Adsorption studies of Zinc (II) on magnetite, baobab (*Adensonia digitate*) and magnetite-baobab composite. *Journal of applied water Sciences, 8*:222. [Crossref]

Abisola E., Blessed S., Kayode A., (2020). Adsorption of Lead ions on magnetically separable Fe_3O_4 watermelon composite. *Journal of Applied Water Science,* 10:225. [Crossref]

Abrishamkar M., Andayesh R., Hodaee H. (2020). Optimization of important factors on adsorption of methyl violet by modified palm fiber using experimental design method. *Advanced Journal of Chemistry-Section A,* 3(3):237-254. [Crossref]

Ali N.S., Jabbar N.M., Alardhi S.M., Majdi H.S., Albayati T.M., (2022). Adsorption of methyl violet dye

onto a prepared bio-adsorbent from date seeds: Isotherm, kinetics, and thermodynamic studies. *Heliyon*, 8(8):e10276. [Crossref]

Anisuzzaman S.M., Joseph G.C., Daud A.M.S.B.W., Krishnaiah D., Yee H.S., (2015). Preparation and characterization of activated carbon from typha orientalis leaves. *International Journal of Industrial Chemistry*, 6:9-21. [Crossref]

Ayuba A.M., Hamisu A., (2022). Raw water lily leaves (*Nymphaea Lotus)* poder as an effective adsorbent for adsorption of malachite green dye from aqueous solution. *Chemical Review and Letters,* 5:250-260. [Crossref]

Ayuba A.M., Thomas N.A., (2019). Paraquat dichloride adsorption from aqueous solution using carbonised Bambara groundnut (vigra subterranean) shells. *Bayero journal of pure and applied sciences,* 12(1):167-177. ISSN 2006-6996. [Crossref]

Bedmohata M.A., Chaudhari A.R., Singh S.P., Choudhary M.D., (2015) Adsorption capacity of activated carbon prepared by chemical activation of Lignin for the removal of methylene blue dye. *International Journal of advanced Research in Chemical Science (IJARCS),* 2(8):1-13.

Belala Z., Jeguirin M., Belhachemi M., Addoun F., Trouve G., (2011). Biosorption of basic dye from aqueous solutions by date stones and palm-trees waste: kinetic, equilibrium and thermodynamic studies. *Desalination,* 271:80-87. [Crossref]

Bonetto L.R., Ferrarini F., De Marco C., Crespo J.S., Guegan R., Giovanela M., (2015) Removal of Methyl Violet 2B from aqueous solution using a magnetic composite as adsorbent. *Journal of Water Process Engineering, Elsevier,* 6:11-20. [Crossref]

Chakraborty S., Chowdhury S., Saha D.P., (2011). Adsorption of crystal violet from aqueous solution ontoNaOH-modified rice husk.*Carbonhydrate Polymers,* 86:1533-1541. [Crossref]

Dahri M.K., Kooh R.R.M., Lim L.B.L., (2013). Removal of Methyl Violet 2B from aqueous solution using *casuarina equisetofolia* Needle. *Hindawi* Publishing Corporation ISRN Environmental Chemistry, 1-9. [Crossref]

Dehgani M.H., Farhang M., Alimohammadi M., Afsharnia M., Mckay G., (2018). Adsorptive removal of fluoride from water by activated carbon derived from CaCl2-modified cracus sativus leaves: Equilibrium adsorption isotherms, optimization and influence of anions. *Chemical Engineering Communications,* 205(7):955-965. [Crossref]

Duan J., Liu J., Chen T., Zhang B., Liu J., (2012). Halloysite nanotube-Fe_3O_4 composite for the removal of methyl violet from aqueous solution. *Desalination,* 293:46-52. [Crossref]

Foroutan R., Mohammadi R., Ahmadi A., Bikhabar G., Babaei F., Ramavandi B., (2022). Impact of ZnO and Fe3O4 magnetic nanoscale on the methyl violet 2B removal efficiency of the activated carbon oak wood. *Chemosphere*, 286:131632. [Crossref]

Geremew B., Zewde D., (2022). Hagenia abyssinica leaf powder as a novel low-cost adsorbent for removal of methyl violet from aqueous solution: Optimization, isotherms, kinetics, and thermodynamic studies. *Environmental Technology & Innovation*, *28*: 102577. [Crossref]

Giwa S.O., Moses J.S., Adeyi A.A., Giwa A., (2018). Adsorption of atrazine from aqueous solution using desert date seed shell activated carbon. *ABUAD Journal of engineering research and development (AJERD),* 1(3):317-325.

Hameed, B. H., & El-Khaiary, M. I. (2008). Sorption kinetics and isotherm studies of a cationic dye using agricultural waste: Broad bean peels. *Journal of Hazardous Materials, 154*(1), 639–648. [Crossref]

Ibrahim M.B., Sani S., (2015). Neem (*Azadirachta Indica*) leaves for the removal of organic pollutants. *Journal of Geosciences and Environmental protection,* 3:1-9. [Crossref]

Karim B.A., Mounir B., Hachkar M., Bakasse M., Yaacoubi A., (2017). Adsorption/Desorption behaviour of cationic dyes on Moroccan Clay: equilibrium & Mechanism. *Journal of Materials and Environmental Sciences*. 8(3):1082-1096. [Crossref]

Kayode A., Abisola E., Blessed S., (2020). Adsorption of Lead ions on magnetically separable Fe3O4 watermelon composite. *Applied water Sciences,* 10(225):1-8. [Crossref]

Li C., Zhang X., Pan J., Xu P., Liu Y., Yan Y., Zhang Z., (2010). Strontium (II) ion surface-imprinted polymers supported by potassium tetratitanate whiskers: synthesis, characterization and adsorption behaviours. *Journal of adsorption Science and technology*, 27(9):845-859.

Lofrano G., Carotenuto M., Libralato G., Domingos F.R., Markus A., Dini L., Gautam K.R., Baldantoni D., Rossi M., Sharma K.S., Chattopadhyaya M.C., Giugni M., (2016). Polymer functionalised nanocomposites for metals removal from water and wastewater: An overview. *Water Research,* 92:22-37. [Crossref]

Lu Y.C., Kooh M.R.R., Lim L.B.L., Priyantha N., (2021). Effective and simple NaOH-modification method to remove methyl violet dye via Ipomoea aquatica roots. *Adsorption Science & Technology*, 1-12. [Crossref]

Majithiya D., Yadav A., Tawde S., (2013). Comparative studies of *Azidirachta indica* (Neem) leaf powder and activated carbon as an adsorbent for removal of chromium from an aqueous solution, *Journal of environmental science and sustainability (JESS),* 1(1):21-27. [Crossref]

Malik R., Ramteke D.S., Wate S.R., (2007). Adsorption of malachite green on groundnut shell waste based powdered activated carbon. *Waste Management,* 27(9):1129-1138. [Crossref]

Manjunatha K.R., Vagish M., (2016). Study on adsorption efficacy of neem leaves powder in the removal of reactive red dye colour from aqueous solution. *International Research Journal Engineering & Technology,* 3:12-24.

Mehr H.V., Saffari J., Mohammadi S.Z., Shojaei S., (2020). The removal of methyl violet 2B dye using palm kernel activated carbon: thermodynamic and kinetics model. *International Journal of Environmental Science and Technology*, *17*:1773-1782. [Crossref]

Mittal A., Gupta V.K., Malviya A., Mittal J., (2007). Process of development for the batch and bulk removal and recovery of a hazardous, water-soluble azo dye (Metanil Yellow) by adsorption over waste materials (Bottom Ash and De-Oiled Soya). *Journal of Hazardous Materials,* 151:821-832. [Crossref]

Mohd Din A.T., Hameed H.B., (2010). Adsorption of Methyl violet dye on acid modified activated: Isotherms and thermodynamics. *Journal of applied Sciences in environmental sanitation,* V(N):151-160.

Mohd Din A.T., Yew H.F.C., Malik M.S.A., (2009). A liquid-phase batch adsorption study of methyl violet dye removal using acid modified activated carbon. *16th ASEAN Regional Symposium on Chemical Engineering*, Philippines.

Naghizadeh A., Nasseri S., Nazmara S., (2011). Removal of trichloroethylene from water by adsorption onto multiwall carbon nanotubes. *Iran journal of environmental health science engineering.* 8(4):317-324.

Nica I., Zaharia C., Baron I.R., Coseri S., Suteu D., (2020). Adsorptive materials based on cellulose: preparation, characterization and application of copper ion retention. *Cellulose Chemistry Technology,* 54:5-6. [Crossref]

Nyijime T.A., Ayuba A.M., (2020). Kinetic and equilibrium studies of paraquat dichloride adsorption of raw Bambara groundnut (*Vigna subterranean)* shells. *Applied Journal of environmental engineering,* 6N^0(1):1-13. [Crossref]

Oyeyode O.J., Ayuba A.M., (2022). Adsorption of Methyl Orange Dye from Aqueous Solutions by Carbonised Iron Tree (*Prosopis Africana)* Seeds: Kinetic, Equilibrium & Thermodynamics Studies. *Applied Journal of Environmental Engineering Science*, 8N^0(2):130-147.

Oznur D., Fatma I., Kadir T., Mahmure O., (2013). Sumec leaves as a Novel low cost adsorbent for removal of basic dyes from aqueous solution. *Hindawi publishing corporation (ISRN) analytical Chemistry*, [Crossref]

Samal K., Raj N., Mohanty K., (2019). Saponin extracted waste biomass of Sapindus mukorossi for adsorption of methyl violet dye in aqueous system. *Surfaces and Interfaces*, *14*:166-174. [Crossref]

Sartape S.A., Mandhare M.A., Jadhav V.V., Raut D.P., Anusa A.M., Kolekar S.S., (2017). Removal of malachite green dye from aqueous solution with sorption techniques using *Limonia Acidissima* (wood apple) Shell as low-cost adsorbents. *Arabian Journal of Chemistry,* 10:3229-3238. [Crossref]

Shahryari Z., Goharrizi S.A., Azadi M., (2010). Experimental study of methylene blue adsorption from aqueous solution onto a carbon nanotube. International *Journal of water Resources and environmental engineering.* 2(2):016-028. [Crossref]

Sharafzad A., Tamjidi S., Esmaeili H., (2021). Calcined lotus leaf as a low-cost and highly efficient biosorbent for removal of methyl violet dye from aqueous media. *International Journal of Environmental Analytical Chemistry*, 101(15):2761-2784. [Crossref]

Syakina A.N., Rahmayanti M., (2023). Removal of Methyl Violet from Aqueous Solutions by Green Synthesized Magnetite Nanoparticles with Parkia Speciosa Hassk. Peel Extracts. *Peel Extracts. SSRN*, 7-10. [Crossref]

Ullah S., Ur Rahman A., Ullah F., Rashid A., Arshad T., Viglasova E., Galambos M., Mahmoode M.N., Ullah H., (2021). Adsorption of Malachite green dye onto mesoporous natural inorganics clays:equilibrium isotherm and kinetic studies. *Water*, 13:965. [Crossref]

Yamil L.D.O., Georgin J., Franco D.S., Netto M.S., Grassi P., Piccilli D.G., Dotto G.L., (2020). Powdered biosorbent from pecan pericarp (Carya illinoensis) as an efficient material to uptake methyl violet 2B from effluents in batch and column operations. *Advanced Powder Technology*, 31(7):2843-2852. [Crossref]

You X., Zhou R., Zhu Y., Bu D., Cheng D., (2022). Adsorption of dyes methyl violet and malachite green from aqueous solution on multi-step modified rice husk powder in single and binary systems: Characterization, adsorption behavior and physical interpretations. *Journal of Hazardous Materials*, *430*:128445. [Crossref]

Yusuff S.A., (2019). Adsorption of hexavalent Chromium from aqueous solution by *Leucaena leucocephala* seed pod activated carbon: equilibrium, kinetics and thermodynamics studies. *Arab Journal of Basic and Applied Sciences,* [Crossref]

Zhai H., Zou J., Liu F., Han X., Zhou W.J., (2020). Adsorption removal of methylviolet from aqueous solution by chromium phosphovanadate. *Surface Interface Analysis. 53:76-83.* [Crossref]

Zubair M., Mu'azu N.D., Jarrah N., Blaisi N.I., Aziz H.A.A., Al-Harthi M., (2020). Adsorption behavior and mechanism of methylene blue, crystal violet, eriochrome black T, and methyl orange dyes onto biochar-derived date palm fronds waste produced at different pyrolysis conditions. *Water, Air, & Soil Pollution. 231*:1-19. [Crossref]